NUCLEAR STRUCTURE
(EXPERIMENTAL)

THE MASS OF ^{59}ZN

B. Sherrill, K. Beard, W. Benenson, B.A. Brown, E. Kashy, W.E. Ormand, H. Nann[+], J.J. Kehayias[+], A.D. Bacher[+], and T.E. Ward[+]

I. Introduction

The nucleus 59Zn is the heaviest T_z=-1/2 nucleus for which the mass and lifetime are known. This makes it important for mass predictions and calculations of Gamow-Teller matrix elements in nuclear beta decay. The mass measurement of 59Zn also represents the first in a series of T=1/2 nuclei in this region of the isotope table which are needed to extend the Garvey-Kelson charge symmetric mass predictions(1) to A>56. Further, since the mass of the T_z=1/2 mirror nucleus is known, the Coulomb energy shift systematics can be extended to the A=59 mirror pair.

This measurement is the first use of the (p,π-) reaction to measure a nuclear mass. The (p,π-) reaction allows a considerably more accurate (<50 kev) mass measurement than the beta-endpoint technique commonly used to make mass measurements of proton rich nuclei.

II. Method

The measurement was performed at the Indiana University Cyclotron Facility (IUCF) with a proton beam of 190 MeV. The QQSP spectrometer(2) set at 30 degrees was used to determine the outgoing pion kinetic energy. At the focal plane of the spectrometer a vertical drift chamber detector measured both position and angle(3). Figure 1 shows the spectrograph and detector layout. The standard setup, which is described in reference 3,

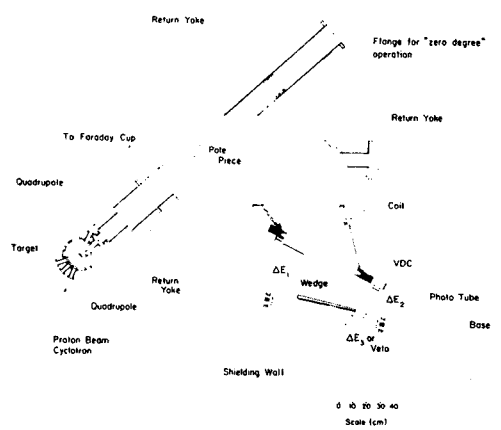

Fig. 1 Diagram showing the QQSP spectrograph. The alumimun wedge was used to stop the pions in the second scintillator.

uses time of flight between the scintillators and between the front scintillator and the rf of the cyclotron to eliminate background from other particles, particularly electrons. In the present experiment an aluminum absorbing wedge was placed after the focal plane detector and before the scintillators, as shown in the fig. 1. The thickness of the wedge was chosen to cause the negative pions to stop in the second scintillator, where they deposited some part of their rest mass energy plus their kinetic energy. Thus, by gating on large (E > 40 MeV) energy signals in the back scintillator we were able to reduce the background by two orders of magnitude without changing the efficiency. The limitation of this technique is that it works for only a limited range of pion energy due to the geometry of the wedge and the pion orbits in the spectrograph.

The mass measurement itself was carried out by determining the Q-value of the reaction 58Ni(p,π-)59Zn relative to the Q-values of the calibration reactions(4)

13C(p,π-)14O (g. s.)	Q= -136.650 MeV
25Mg(p,π-)26Si (1.796 MeV)	Q= -140.595 MeV
25Mg(p,πs)26Si (2.783 MeV)	Q= -139.607 MeV

Since the QQSP measured angle as well as position, the 14O calibration runs could be divided into 11, 0.9 deg. angular bins. This gave a calibration point every channel in the region of the 59Zn ground state and provided a precise calibration of spectrograph focal plane. Calibration runs of 14O were taken before and after each 59Zn run to monitor changes in the proton beam energy. The same spectograph parameters were used for all runs. Finally, the target thicknesses were chosen so the energy loss corrections were the same in each target, within 14keV, for the reactions studied.

III. Results

The Q-value for the 58Ni(p,π-)59Zn reaction was measured to be Q= -145.247(40) MeV, which gives a mass excess of ME(59Zn)= -47.256(40) MeV. The measured cross section was 0.080(20) nb/sr. This mass compares favorably to the beta-endpoint measurement made by Arai et.al.(5) of ME(59Zn)= -47.23(10) MeV. The weighted average of the two measurements is ME(Zn59)= -47.253(37) MeV. The experimental spectrum is shown in figure 2 along with a calibration spectrum. The 58Ni target data is integrated over the whole angular range (10.8 deg) whereas the 13C spectrum is shown for a 1 deg acceptance.

The uncertainty in the mass measurement of 59Zn came from four sources. First, the difference in reaction kinematics between 58Ni(p,π-) and the calibration reactions 13C(p,π-) and 25Mg(p,π-) coupled to a 0.5 degree uncertainty in spectrograph angle lead to a 20 keV systematic uncertainty in the measurement. Second, the absolute beam energy is known to 200 keV. This lead to a 4 keV uncertainty, again due to the difference in reaction kinematics. Third, beam energy fluctuations observed were of the order of 80 keV. Thus, although the 59Zn runs were shifted and summed according to the observed shifts in the calibration spectra, we

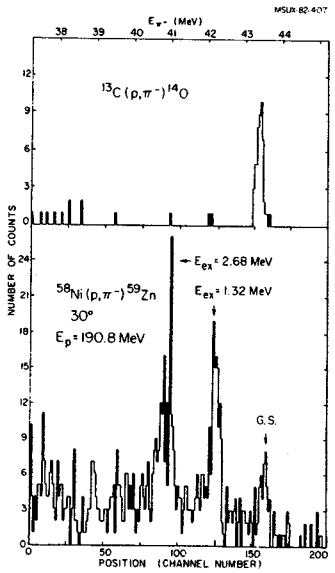

Fig. 2 Spectrum showing the focal plane position (channel number) vs. the number of observed counts for the 59Zn mass measurement and the 140 calibration.

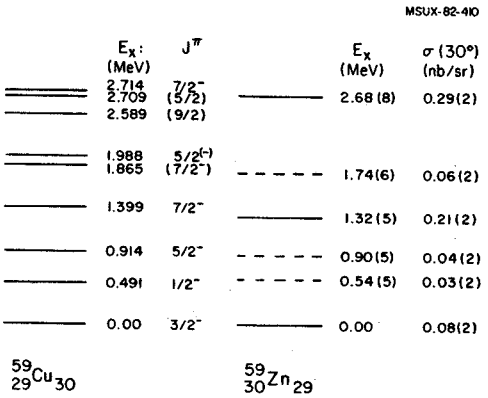

Fig. 3 The level structures of the mirror pair 59Zn-59Cu. The ground states are offset in excitation energy to allow comparison of level spacing.

conservatively estimated that this fluctuation introduced a 20 keV systematic uncertainty into the mass measurement. Finally, low statistics, due to the small 58Ni(p,π-) cross section and background subtraction, lead to a 28 keV uncertainty. All other contributions to the uncertainty were determined to be less than 4 keV. For the final total uncertainty all effects were added in quadrature.

The measured low lying level structure of 59Zn is shown in figure 3. Also shown is the level structure of 59Cu(6), mirror nucleus of 59Zn. The cross sections are consistent with the observation that the (p,π-) reaction selects high spin states due to the pion/proton momentum mismatch(7).

The ft-values for the B+ decay of 59Zn have been calculated previously(5,9). Using the new mass of 59Zn we obtained a more accurate value for the decay to the ground state 59Cu. The statistical rate function f was calculated, using the method of reference 8, to be f=25627(848). About one third of the error is from the extension of the parameters in reference 8 to all isotopes of a given Z. The remaining error in f is due to the uncertainty of the 59Zn mass. Using the weighted average of the lifetime and branching ratios(5,9) we obtain ft=5016(185). For this value to be useful for the study of weak interactions the error should be decreased by at least a factor of three. Also of interest are the ft values of the B+ decays to the excited states in 59Cu. These decays are pure Gammow-Teller transitions. Improvement in their precision might lead to information about weak interactions and nuclear structure effects in weak decays. The main source of error in the decays to the excited states is in the measured values for the branching ratios.

We also attempted to measure the mass of 41Ti with the reaction 40Ca(p,π-), but no counts were observed above the background. This lack of yield gives an upper limit for the cross section of 0.003 nb/sr.

IV. Discussion

Since 59Zn is the heaviest T_z=-1/2 nucleus of measured mass it provides a check on the persistence of the Nolen-Schiffer (N-S) anomaly(10) in higher mass nuclei. The measured Coulomb energy shifts between the 59Zn-59Cu pair are

$$E_c\ (\ 59;\ 7/2^-\ ) = 9810(60)\ \text{keV}$$
$$E_c\ (\ 59;\ 3/2^-\ ) = 9882(40)\ \text{keV}$$

Compairing these measured shifts to the particle-core model of Brown(11), there is a 5% discrepency for the 2p3/2 state and a 7% discrepency for the 1f7/2 state. This is in agreement with lower-mass mirror pair systematics.

The measured mass excess, of 59Zn, is compared to several mass predictions in Table 1. The agreement is typical for this region of the isotope table. Therefore, there appears to be no surprises in the comparison of the measured mass excess to the mass predictions.

The biggest disadvantage of the use of the (p,π-) reaction for mass measurements is the small ground state cross section. This is due to the large negative Q-values and the resulting proton/pion momentun mismatch. This leads to the

Table 1. Comparison of mass excess predictions to the measured value.

Mass Prediction[a]	Mass Excess (MeV)
Myers	- 50.4
Grotte-Hilf-Takahashi	- 47.73
Seeger-Howard	- 48.1
Liran-Zeldes	- 47.33
Beiner-Lombard-Mas	- 45.8
Janecke-Garvey-Kelson	- 47.39
Experimental value	- 47.25 (4)

[a] S. Maripu, special ed., At. Data Nucl. Data Tables 17, 494 (1976).

selection of high spin states in the residual nucleus over the low spin ground state. The failure to observe the ground state of 41Ti in the 40Ca(p,π-) reaction is evidence of this effect. If, however, 40Ca had a large 2p-2h neutron component in the ground state, it would show up in the (p,π-) spectrum. The absence of any observed counts near the expected ground state sets an upper limit of about 25% for the 2p-2h neutron contribution to the 40Ca wave function.

Due to the low cross sections and lack of suitable targets there are not many uses for the (p,π-) reaction in mass measurements. Two remaining posibilities are 64Zn(p,π-)65Ge and 92Mo(p,π-)93Ru. Many more proton rich nuclei could be reached with the (3He,π-) reaction, but the ground state cross sections are expected to be quite small due in part to a momentum mismatch even worse than that of the (p,π-) reaction.

ACKNOWLEDGEMENTS

The authors are greatly indebted to M.C Green and the rest of the IUCF pion group for their help on this experiment.

+ Indiana University Cyclotron, Indiana Univ., Bloomington, IN 47405.

1. I. Kelson and G.T. Garvey, Phys. Lett. 23,689(1966).
2. M.C. Green, Proc. Pion Production and Absorption in Nuclei-1981, (AIP,1982)131.
3. M.C. Green, Phd. Thesis, Indiana Univ., unpublished.
4. A.H. Wapstra and K. Bos, 1982 Atomic Mass Evaluation, Nuclear Data Center, Brookhaven Nat. Lab., unpublished.
5. Y. Arai et al., Phys. Lett. 104B,186(1981).
6. C.M. Lederer and U.S. Shirley, eds., Table of Isotopes (Wiley,1978).
7. B.A. Brown, D. Scholten and H. Toki, to be published.
8. D.H. Wilkinson and B.E.F. Macefield, Nuc. Phys. A232,58(1974).
9. J. Honkanen et al., Nuc. Phys. A366,109(1981).
10. J.A. Nolen Jr. and J.P. Schiffer, Ann. Rev. of Nuc. Sci. 19,471(1969). 11
11. B. Sherrill et. al., Phys. Rev. C28, 1712 (1983).

^{154}Sm(p,p') REACTIONS AT 35, 65, AND 134 MEV

R.M. Ronningen

During this past year we have completed coupled channels analyses of ^{154}Sm(p,p') reactions at 35 MeV (data from MSU[1]), 65 MeV (data from the University of Maryland[2]), and 134 MeV (data from the Indiana University Cyclotron Facility[3]). Proton scattering data at 51[4] and 800 MeV[5] also exist. Thus, sufficient data on this reaction make possible energy-dependence systematic studies of the deformation parameters and multipole moments. Regarding the former, from the analyses of the 35, 65, and 134 MeV data we have found the hexacontatetrapole deformation parameter to be positive in each case. The deformation lengths of the real potentials, $\beta_6 r_o$, average to about 0.008 fm.

Brieva and Georgiev[6] have pointed out that because of the energy dependence of the deformed optical model potential derived from a realistic nucleon-nucleon interaction, the moments of the potential derived from a standard phenomenological optical model analysis should show an energy dependence. This energy dependence is expected to increase with multipole moment order and is also greater for moments extracted from the imaginary part of the potential.

In Fig. 1 we show the percentage variation of multipole moments of the potentials with respect to those of the underlying nucleon density for proton scattering at 35, 51, 65, and 134 MeV. (The calculations are those of Brieva and Georgiev.) The percentage variation is defined as

$$Q^{R,I}_{\lambda o}(E) = \frac{q^{R,I}_{\lambda o}(E) - q^{D}_{\lambda o}}{q^{D}_{\lambda o}} \times 100\%$$

where $q^{R,I}_{\lambda o}(E)$ are the multipole moments (normalized to mass) of the real and imaginary parts of the phenomenological potential used to fit the scattering data at each energy, and $q^{D}_{\lambda o}$ are the moments used by Brieva and Georgiev - (q^{D}_{20} = 5.211 b, q^{D}_{40} = 1.173 b^2, q^{D}_{60} = 0.162 b^3).

Except for Q^{R}_{20} at 35 MeV and Q^{R}_{40} at 65 MeV the predicted energy dependence for Q^{R}_{20} and Q^{R}_{40} are followed remarkable well, given that the underlying density is correct. Comparisons for Q^{R}_{60} are not made. The theoretical analysis and the analysis of the 51 MeV data used a negative value of β_6 (the omission of a β_6 value of the order we observe affects q^{R}_{40} by about 5% and Q^{R}_{40} by 20%-30%). We conclude that the observed energy dependence of the moments may signify that there is not a simple relation between the moment of the optical potential and the moments of the matter density, and perhaps density-dependent interactions are being observed. However, this conclusion should be tested for more systems.

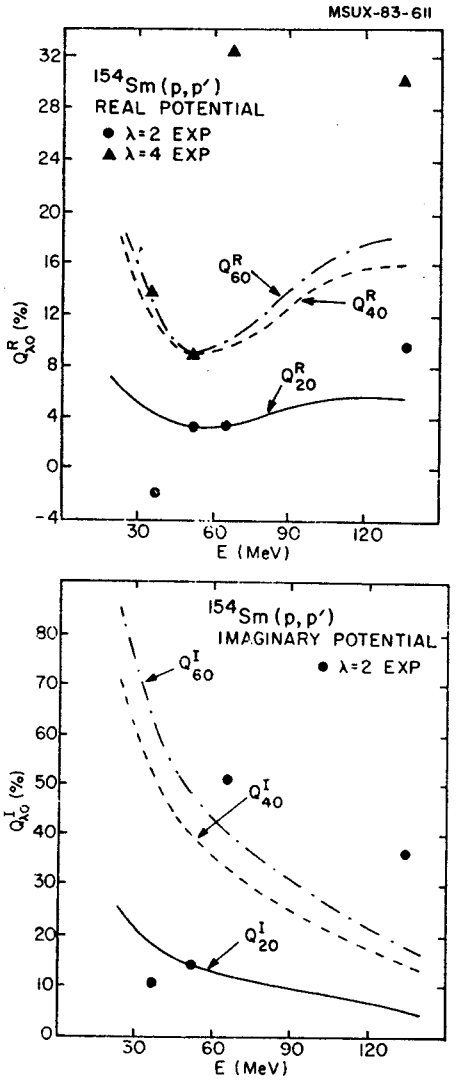

Fig. 1. Comparisons of the percentage differences between experimental multipole moments (closed symbols) from (p,p') reactions and those of a microscopically calculated potential having an underlying density with given multipole moments as a function of incident proton energy. The $Q^{R,I}_{\lambda o}(E)$ are defined in the text.

1. R.M. Ronningen, G.M. Crawley, J.A. Nolen, and R.C. Melin, unpublished.
2. R.M. Ronningen, P.H. Debenham, A. Gutermann, D.L. Hendrie, and A. Nadasen, Michigan State University Cyclotron Laboratory Annual Report, p. 40 (1982).
3. R.M. Ronningen, G.M. Crawley, N. Anantaraman, S.M. Banks, B.M. Spicer, G.G. Shute, V.C. Officer, J.M.R. Wastell, D.W. Devins, and D.L. Friesel, Phys. Rev. C 28, (1983).
4. P.B. Woollam, R.J. Griffiths, F.G. Kingston, C.B. Fulmer, J.C. Hafele, and A. Scott, Nucl. Phys. A179, 657 (1972).
5. M.L. Barlett, J.A. McGill, L. Ray, M.M. Barlett, G.W. Hoffmann, N.M. Hintz, G.S. Kyle, M.A. Franey, and G. Blanpied, Phys. Rev. C 22, 1168 (1980).
6. F.A. Brieva and B.Z. Georgiev, Nucl. Phys. A308, 27 (1978).

^{154}Sm, ^{166}Er, ^{176}Yb, $^{182}W(\vec{p},p')$ REACTIONS AT 134 MeV

R.M. Ronningen, N. Anantaraman, G.M. Crawley, P. Andrews*, S.M. Banks*, V.C. Officer*, G.G. Shute*, B.M. Spicer*, J.M.R. Wastell*, D.W. Devins***, R.P. DeVito**, and D.L. Freisel**.

Our study of the ^{154}Sm, ^{166}Er $(\vec{p},p')$ reactions at 134 MeV is just now published.[1] The cross section and asymmetry data are well described by a coupled channels analysis for scattering from a deformed optical model potential within a rigid rotor model framework. The angular distributions of cross sections were also investigated using an analytic eikonal approximation model developed by Amado and co-workers[2], from which satisfactory descriptions were obtained as well as insight into the relative contributions of single-step and multi-step excitations.

We also found that the multipole moments of the real potential were in good agreement with measurements using other reactions but that there might be slight energy dependences. The hexacontatetrapole deformation parameter, β_6, was found to be positive for ^{154}Sm and negative for ^{166}Er, in agreement with the predictions by Nilsson et al.[3]

To investigate further the trend of β_6 in this mass region as well as other coupled channel effects we have extended our study to ^{176}Yb and ^{182}W using the same reaction. Elastic and inelastic scattering measurements were made using the 134 MeV polarized proton beam from the Indiana University Cyclotron Facility. The scattered particles were detected by a helical-wire position-sensitive proportional counter in the focal plane of the QDDM spectrometer. Angular distributions of cross sections and asymmetries for ground band states having $J^\pi=0^+$ through 8^+ (6^+ in the case of ^{182}W) were measured at laboratory angles from 22° through 42° in 2° steps and then through 77° (^{176}Yb) or 79.5° (^{182}W) in 2.5° steps. Typical spectra are shown in Figure 1. All spectra are now being reduced to obtain cross sections and asymmetries. Coupled channels analyses will then begin.

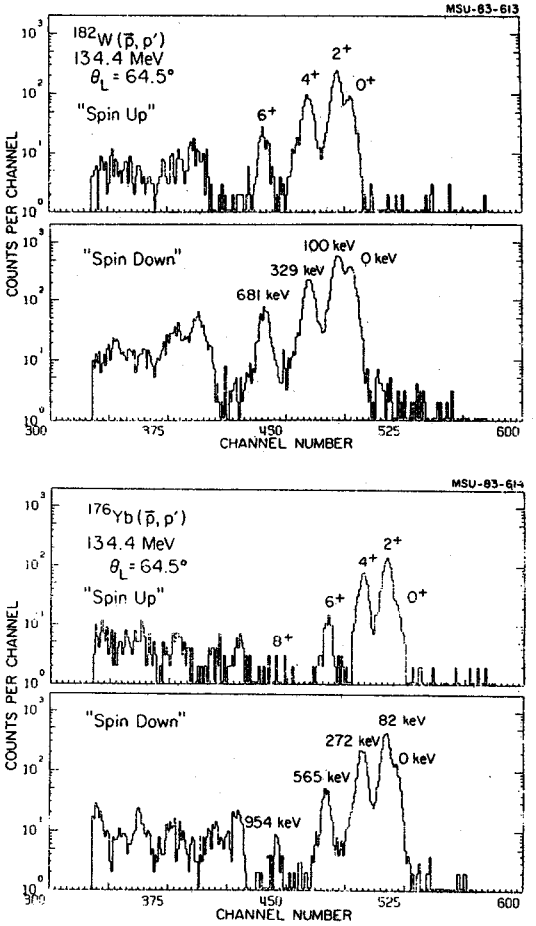

Fig. 1. Spectra from the ^{176}Yb, $^{182}W(\vec{p},p')$ reactions at 134 MeV. "Spin Up" and "Spin Down" data are shown for $\theta_{lab}=64.5^o$.

* University of Melbourne, Parkville, Victoria, Australia 3052.
** Indiana University Cyclotron Facility, Bloomington, IN 47401.
*** Present address: Koppers Process Technology, Norcross, GA 30093.

1. R.M. Ronningen, G.M. Crawley, N. Anantaraman, S.M. Banks, B.M. Spicer, G.G. Shute, V.C. Officer, J.M.R. Wastell, D.W. Devins and D.L. Freisel, Phys. Rev. C 28, 123(1983).
2. R.D. Amado, J.A. McNeil, and D.A. Sparrow, Phys. Rev. C 25, 13 (1982) and references therein.
3. S.G. Nilsson, Chin Fu Tsang, A. Sobiczwski, Z. Szymanski, S. Wychech, C. Gustafson, I.-L. Lamm, P. Möller and B. Nilsson, Nucl. Phys. A131, 1 (1969).

EXCITATION OF ℓ=0, SPIN-FLIP TRANSITIONS BY INELASTIC SCATTERING OF 201 MeV PROTONS.

N. Anantaraman, G.M Crawley, J. Duffy, A. Galonsky, C. Djalali*, J.-C. Jourdain*, N. Marty*, M. Morlet*, and A. Willis*.

At high bombarding energies and very forward angles, the inelastic scattering of protons strongly excites ℓ=0, spin-flip (M1) transitions. This fact has enabled us to successfully study the M1 strength distribution in over two dozen nuclei using the 201-MeV proton beam of the Orsay synchrocyclotron, coupled with the highly developed detection system of the spectrometer magnet used. The results on nuclei from A=40 to A=140 have been reported in the last two Annual Reports. In the past year, we have studied some more nuclei in this mass range, and also extended the measurements to both lighter nuclei (^{24}Mg, ^{28}Si) and heavier nuclei (^{208}Pb). A summary of the work done in the past year follows.

(A) The N=28 Isotones ^{48}Ca, ^{50}Ti, ^{52}Cr, ^{54}Fe

This work has been completed and two papers submitted for publication--one[1] on ^{48}Ca and the other[2] on the rest of the nuclei. ^{48}Ca shows an extreme concentration of M1 strength: observations down to 2° reveal $0^+ \rightarrow 1^+$ strength with certainty only at the previously known excitation of 10.2 MeV (see top part of Fig. 1). Compared to microscopic distorted-wave impulse approximation calculations, the strength of the 10.2-MeV state is only 30% of that expected. This quenching is qualitatively consistent with that observed in (p,n), (e,e') and other (p,p') measurements on ^{48}Ca.

The effect of adding protons in the $1f_{7/2}$ shell to ^{48}Ca is shown in the lower three spectra of Fig. 1. For all the targets, nearly all the states observed at small angles between 8 and 15 MeV excitation have forward-peaked angular distributions well fitted by an ℓ=0 shape. A comparison with $(\vec{\gamma},\gamma)$ results demonstrates the 1^+ nature of the states[2]. As one moves from ^{48}Ca to ^{50}Ti, the single state at 10.2 MeV in ^{48}Ca, which presumably arises from the neutron excitation $f_{7/2} \rightarrow f_{5/2}$, splits up into a number of different states near 8.5 MeV, which is predicted by the shell-model calculations of Metsch and Knupfer to arise mainly from proton excitations. In ^{52}Cr and ^{54}Fe, the strength is more widely spread between 8 and 12 MeV. The ratio of experimental to predicted cross sections ranges from 0.25 for ^{50}Ti to 0.44 for ^{54}Fe.

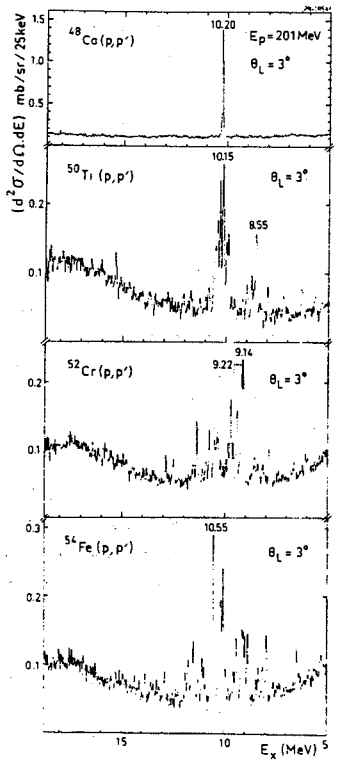

Fig. 1. Spectra of protons inelastically cattered from ^{48}Ca, ^{50}Ti, ^{52}Cr, and ^{54}Fe at 3°.

(B) The Ca Isotopes ^{40}Ca, ^{42}Ca, ^{44}Ca, ^{48}Ca

Fig. 2 shows spectra measured at 3° for ^{40,42,44,48}Ca. The ^{40,48}Ca data have been reported previously. The ^{42,44}Ca spectra have some oxygen and carbon peaks, the strong ones being identified by the symbols O and C, respectively. They served as internal energy

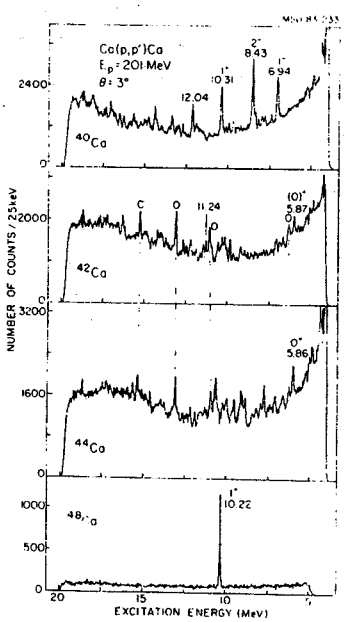

Fig. 2. Spectra of protons inelastically scattered from ^{40}Ca, ^{42}Ca, ^{44}Ca and ^{48}Ca at 3°.

calibration points. A comparison with back-angle Ca(e,e') measurements, where these states were first observed,[3] has been made. Whereas only a single 1^+ state was strongly excited in ^{42}Ca(e,e'), the (p,p') reaction finds four states which have forward-peaked angular distrbutions and which therefore could be 1^+ states (Fig. 3). The two states at 10.08 and 10.24 MeV could be the parents of a 1^+ peak seen in the ^{42}Ca(p,n) reaction[4]. In ^{44}Ca(p,p'), there are seven states with forward-peaked angular distributions, all having roughly similar cross sections (Fig.4). A large fragmentation of the ^{44}Ca M1 strength is found also in the (e,e') reaction.

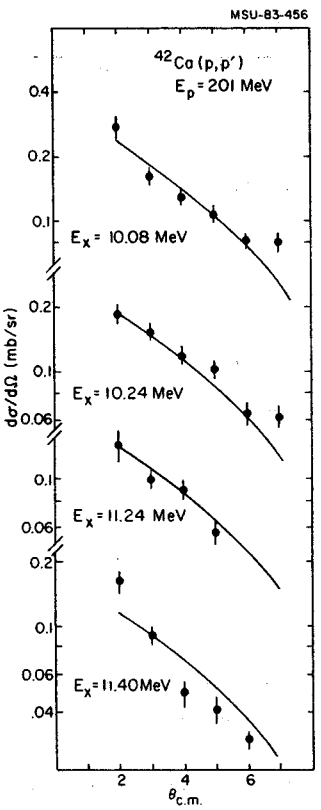

Fig. 3. Angular distributions of possible 1^+ states observed in ^{42}Ca(p,p'). The solid curve represents a smooth line drawn through the data points of the measured 1^+ angular distribution for the strong 1^+ state at 10.22 MeV in ^{48}Ca.

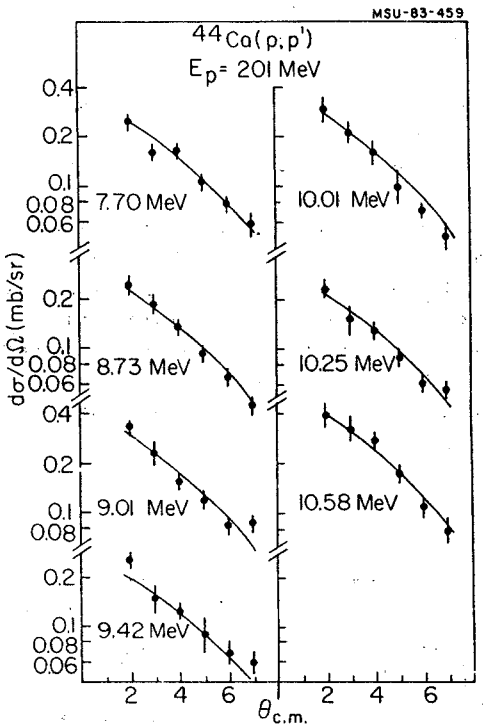

Fig. 4. Same as Fig. 3, but for ^{44}Ca(p,p').

Table 1

Comparison of (p,p') and (e,e') data on the Ca isotopes with the shell-model preditions of ref. 5.

Nucleus	^{40}Ca	^{42}Ca	^{44}Ca	^{48}Ca
$\sum\sigma(p,p')_{3^\circ}$ in mb/sr	0.35/0.6*	0.5	1.5	4.5
$\sum B(M1)\uparrow$(e,e') in μ_o^2	1.12	1.2	2.1	3.7
$\sum B(M1)\uparrow_{theory}$ in μ_o^2	0.0	1.86	4.02	8.58

* depending on whether or not the state at 12.04 MeV is included.

Table 1 compares the (p,p') and (e,e') results for the Ca isotopes with the theoretical predictions of McGrory and Wildenthal[5]. The experimental values are those obtained by summing all the 1^+ states in each nucleus, except in the case of ^{48}Ca (where they are for the single strong state). Even though there are large uncertainties in the summed cross sections for both reactions, the ratio of (p,p') to (e,e') strength seems to show a definite tendency to increase with increasing A. Differences in the results obtained with the two reactions are doubtless party due to the core excitation contribution present for ^{40}Ca and ^{42}Ca. This core excitation is responsible for the entire M1 strength in ^{40}Ca and for part of the strength in ^{42}Ca, and is not included in the theoretical calculation.

(C) The sd-Shell Nuclei ^{24}Mg, ^{28}Si

The ^{24}Mg (p,p') data are presently being analyzed at Orsay. In ^{28}Si, eight isovector (T=1)

levels are known from (e,e') measurements[6]. In the (p,p') study, we observe these levels and a nineth one that is not seen in (e,e'). The angular distributions for seven of these levels are shown in Fig. 5. We have matched these with levels calculated with the new mass-dependent, universal sd-shell Hamiltonion of Wildenthal. The corresponding quenching factors, $\sigma_{exp}/\sigma_{calc}$ for (p,p') and $B_{exp}(M1)/B_{th}(M1)$ for (e,e'), are shown in Table 2. The model predicts only one strong isoscalar 1^+ level; this has been identified at 9.50 MeV excitation in our spectra and is included in Table 2. Because this state is isoscalar, its non-observation in (e,e') is to be expected; the entry in Table 2 for its predicted B(M1) is only $0.031\ \mu_o^2$.

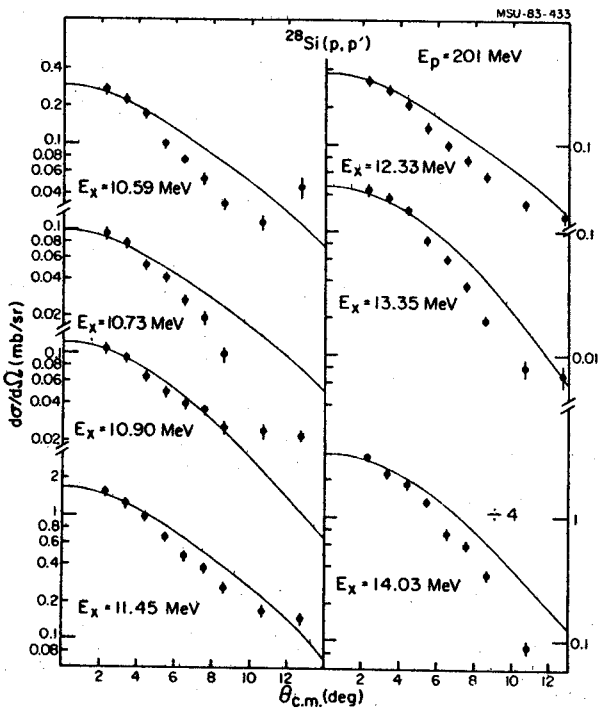

Fig. 5. Angular distributions of isovector 1^+ levels excited in ^{28}Si (p,p'). The solid curves are results of microscopic DWIA calculations normalized to fit the data.

(D) ^{208}Pb

With continued improvement in the beam tuning conditions at the Orsay synchrocyclotron, the slit-scattering contribution to the tail of the elastic peak was reduced sufficiently in our latest run to see clearly the isoscalar 1^+ state at 5.84 MeV excitation in ^{208}Pb. A spectrum at 3° is shown in Fig. 6. The 5.84-MeV state has been the subject of much discussion recently. We hope to study this level quantitatively and also to set an upper limit to the total M1 strength observed in ^{208}Pb(p,p') at 200 MeV.

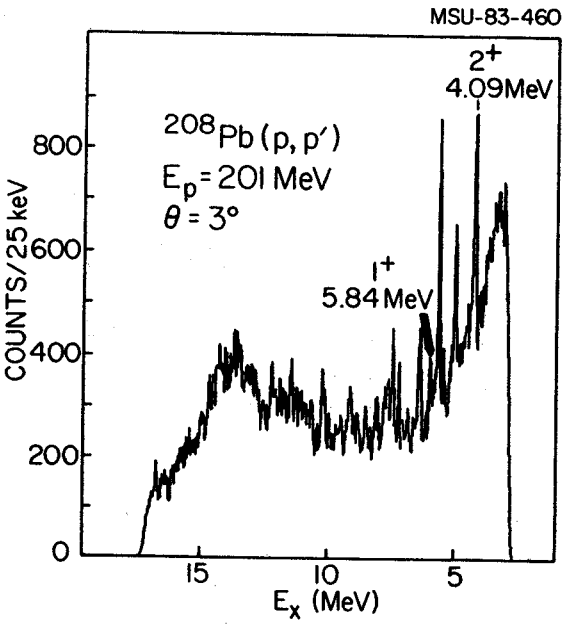

Fig. 6. Spectrum of ^{208}Pb(p,p') at 3°. The isoscalar 1^+ level at 5.84 MeV is indicated.

TABLE 2.

Results for 1^+ levels in ^{28}Si

E_x(exp) (MeV)	E_x(th) (MeV)	$\sigma^{exp}_{p,p'}(0°)$[a] (mb/sr)	$B_{exp}(M1)\uparrow$ (μ_o^2)	$B_{th}(M1)\uparrow$ (μ_o^2)	N	Y^2
9.50[b]	9.40	0.25	–	.031	0.32	–
10.59	10.81	0.30	0.19	1.52	0.20	0.22
10.73		0.12	0.15			
10.90	11.19	0.13	0.68	0.54	0.62	1.26
11.45	11.52	1.65	4.07	3.06	0.72	1.33
12.33	12.64	0.37	0.81	1.39	0.19	0.58
13.35	13.37	0.26	–	0.01	0.58	–
14.07	14.38	0.80	–	0.92	0.40	–
Sum of all levels		3.62	5.90	6.54	0.37	0.90

[a] Extrapolated on the basis of fit to calculated angular distribution.

[b] Isoscalar state. All other levels are isovector in character.

* Institut de Physique Nucléaire, Orsay, France.

1. G.M. Crawley, N. Anantaraman, A. Galonsky, C. Djalali, N. Marty, M. Morlet, A. Willis, and J.-C. Jourdain, Phys. Lett. 127B, 322(1983)
2. C. Djalali, N. Marty, M. Morlet, A. Willis, J.-C. Jourdain, N. Anantaraman, G.M. Crawey, A. Galonsky, and J. Duffy, Nucl. Phys. A (submitted).
3. W. Steffen, H.-D. Graf, W. Gross, D. Meuer, A. Richter, E.Spamer, O. Titze, and W. Knupfer, Phys. Lett. 95B, 23 (1980).
4. C.D. Goodman, C.C. Foster, D.E. Bainum, S.D. Bloom, C. Gaarde, J. Larsen, C.A. Goulding, D.J. Horen, T. Masterson, S. Grimes, J. Rapaport, T.N. Taddeucci, and E. Sugarbaker, Phys. Lett. 107B, 406 (1981).
5. J.B. McGrory and B.H. Wildenthal, Phys. Lett. 103B, 173 (1981).
6. R. Schneider, A. Richter, A. Schwierczinski, E. Spamer and O. Titze, Nucl. Phys. A323, 13 (1979); and A. Richter, in "Nuclear Structure", edited by K. Abrahams, K Allaart, and A.E.L. Dieperink, (Plenum Press, New York, 1981), p. 241

THE (p,n) REACTION ON GAS TARGETS-^{20}Ne and ^{84,86}Kr

R.P. DeVito*, S.M. Austin**, U. Berg***, C.C. Foster*, A. Galonsky**, C.D. Goodman*, B. Remington**, and T.N. Taddeucci+

In many cases (p,n) cross sections and strengths of M1 transitions to analogous states are closely proportional, but this is not always so. Indeed, the operators for these two types of transition depend on spin, but the M1 operator also has an orbital part. That difference has a large effect in A=20 nuclei where a comparison of a $0^+ \rightarrow 1^+$ transition in ^{20}Ne(e,e')^{20}Ne and in ^{20}Ne(π,γ)^{20}F indicates[1,2,3] that spin and orbital (current) contributions are comparable. (The (π^-,γ) reaction is not sensitive to convection currents). Unfortunately the (π^-,γ) data are relatively imprecise. We, therefore, undertook a study of the ^{20}Ne(p,n) reaction to permit a more reliable determination of the relative strengths of the spin and orbital contributions to this transition. We have also made a detailed comparison of our results with the Chung-Wildenthal shell model of these transitions.

The experiment was performed at Indiana University with a beam of 120-MeV protons and the standard beam swinger, time-of-flight facility[4] there. The only significant change was the use of a two-inch long gas target especially constructed for that facility. With 1/2-mil kapton windows the target was usable with pressures up to four atmospheres.

A spectrum taken with a flight path of 100m is shown in Fig. 1. For each of the indicated peaks an angular distribution was determined from 0° to approximately 3.5° and compared to a theoretical angular distribution calculated in the DWIA. Where the spin and parity are known, 2^+ for the ground state and 1^+ for the 0.97-MeV state of ^{20}Na, the measured and theoretical angular distributions agree well. The shape for the next two states, the ones at 1.32 and 1.81 MeV, is characteristic of an L=1 transfer. The theoretical shapes for $J^\pi = 0^-, 1^-$, and 2^- are shown with the data in Fig. 2; comparison rules out a 0^- assignment for these states. Use of another reaction, resonance fluorescence of γ rays[5], rules out 1^- since no E1 strength was observed for these two states. Hence, the two reactions combined require 2^-.

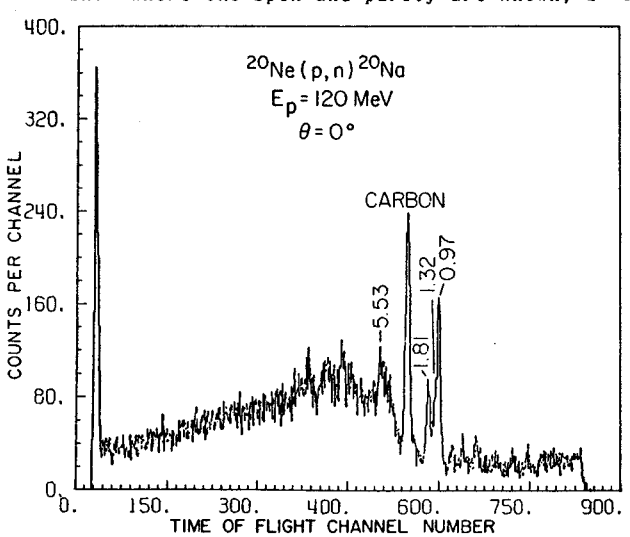

Fig. 1. Neutron spectrum from bombardment of ^{20}Ne gas target with 120-MeV protons. The flight path was 100m.

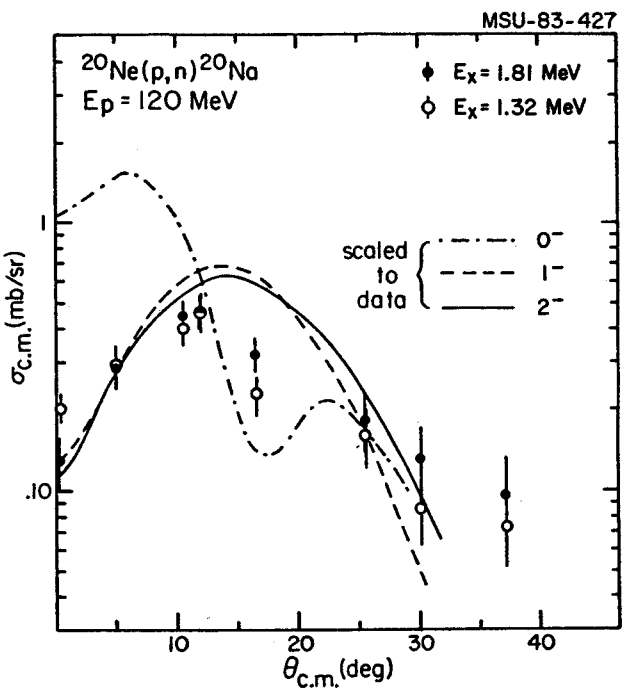

Fig. 2. Measured and computed angular distributions for (p,n) excitation of states of ^{20}Na at 1.29 and 1.79 MeV excitation energy.

The state at 0.973 MeV in ^{20}Na is the isobaric analog of one seen in ^{20}Ne in (e,e') and by resonance fluorescence and in ^{20}F by (π^-,γ). All experiments are consistent with a 1^+ assignment. In the electron and proton induced $0^+ \rightarrow 1^+$ transition there are contributions from orbital recoupling and from spin flip, whereas the (π^-,γ) and (p,n) experiments have no orbital contribution. Combining the value of B(M1+) from the photon experiment with the 0° (p,n) cross section measured here we are able to determine the separate orbital and spin-flip contributions to B(M1+); we get 0.46 $\pm$ 0.06, and 0.54 $\pm$ 0.06, respectively. This result is very different from that for nuclei in the p shell and other nuclei in the s-d shell where spin flip is dominant. It is a triumph for the shell model of Chung and Wildenthal[6] that the corresponding model values are 0.51 and 0.49, in excellent agreement with experiment.

The same gas cell has been used with ^{84}Kr and ^{86}Kr in order to study the relationship between first forbidden beta decay and the (p,n) reaction. A proportionality has been well established between the matrix elements for both Fermi and Gamow-Teller allowed beta decay on the one hand and L=0 (p,n) cross sections on the other. The two krypton isotopes are the final states in $2^- \rightarrow 0^+$ β^+ decay from ^{84}Rb and ^{86}Rb, and the ft values are known. Hence, these can be used as test cases if we measure the (p,n) cross sections for the inverse $0^+ \rightarrow 2^-$ transitions. Cases of so-called "unique" first-forbidden beta decay, such as $2^- \rightarrow 0^+$, are particularly suitable for a test because the involve only a single spin-isospin operator. The (p,n) reaction will require a spin flip and an L=1 transfer. Because L=1 the angular distributions will peak near $\theta=10°$, whereas the (p,n) analogs of Fermi and allowed Gamow-Teller decay peak at $0°$. Although the data have not yet been fully analyzed, one can indeed see the 2^- peak. The spectra in Fig. 3 are for ^{84}Kr at $5.3°$ and $9.6°$. The 2^- peak is weak, but in comparison to the 0^+ and 1^+ Fermi and Gamow-Teller peaks it grows with increasing angle.

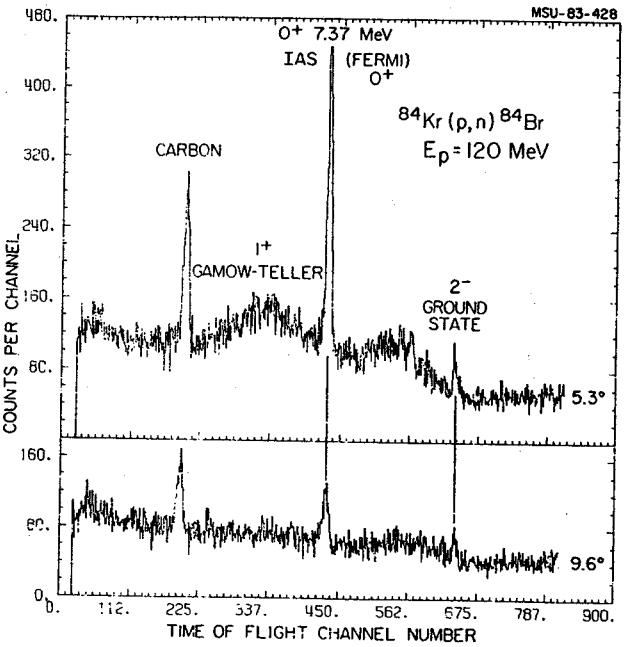

Fig. 3. Neutron time-of-flight spectra from bombardment of the ^{84}Kr gas target with 120-MeV protons. The flight path was 100 m.

* Indiana University Cyclotron Facility
** Michigan State University
*** Justus Liebig University, Giessen
\+ Ohio University

1. W.L. Bendel, L.W. Fagg, S.K. Numrich, E.C. Jones Jr., and H.F. Kaiser, Phys. Rev. C3, 1821 (1971)
2. C. Rangacharyulu et al., Sashatchewan Accelerator Lab 1982 Ann. Report, p. 74
3. C.J. Martoff, J.A. Bistirlich, K.M. Crowe, M. Koike, J.P. Miller, S.S. Rosenblum, W.A. Zajc, H.W. Baer, A.H. Wapstra, G. Strassner, and P. Truol, Phs. Rev. Lett. 46, 891 (1981)
4. C.D. Goodman, C.C. Foster, M.B. Greenfield, C.A. Goulding, D.A. Lind, and J. Rapaport, IEEE Trans. Nucl. Sci. NS26, 2248 (1979)
5. U.E.P. Berg, K. Ackermann, K. Bangert, R. Stock, and K. Wienhard, Phys. Rev. C 27, 2981 (1983)
6. B.H. Wildenthal and W. Chung in The (p,n) Reaction and the Nucleon-Nucleon Force, ed. C. Goodman et al. (Plenum. New York, 1980), p. 89 and private communication